



Missouri University of Science and Technology
Scholars' Mine

International Conferences on Recent Advances
in Geotechnical Earthquake Engineering and
Soil Dynamics

2010 - Fifth International Conference on Recent
Advances in Geotechnical Earthquake
Engineering and Soil Dynamics

29 May 2010, 8:00 am - 9:30 am

Behavior of Model Piles in a Liquefiable Soil in Shaking Table Tests

Chia-Han Chen
National Taiwan University, Taiwan

Tzou-Shin Ueng
National Taiwan University, Taiwan

Follow this and additional works at: <https://scholarsmine.mst.edu/icrageesd>

 Part of the [Geotechnical Engineering Commons](#)

Recommended Citation

Chen, Chia-Han and Ueng, Tzou-Shin, "Behavior of Model Piles in a Liquefiable Soil in Shaking Table Tests" (2010). *International Conferences on Recent Advances in Geotechnical Earthquake Engineering and Soil Dynamics*. 2.

<https://scholarsmine.mst.edu/icrageesd/05icrageesd/session08/2>

This Article - Conference proceedings is brought to you for free and open access by Scholars' Mine. It has been accepted for inclusion in International Conferences on Recent Advances in Geotechnical Earthquake Engineering and Soil Dynamics by an authorized administrator of Scholars' Mine. This work is protected by U. S. Copyright Law. Unauthorized use including reproduction for redistribution requires the permission of the copyright holder. For more information, please contact scholarsmine@mst.edu.



Fifth International Conference on

Recent Advances in Geotechnical Earthquake Engineering and Soil Dynamics and Symposium in Honor of Professor I.M. Idriss

May 24-29, 2010 • San Diego, California

BEHAVIOR OF MODEL PILES IN A LIQUEFIABLE SOIL IN SHAKING TABLE TESTS

Chia-Han Chen

National Taiwan University
Taipei, Taiwan 10617

Tzou-Shin Ueng

National Taiwan University
Taipei, Taiwan 10617

ABSTRACT

The responses of model piles in a liquefiable ground under one- and two-dimensional shakings were studied in a physical model test using a large biaxial laminar shear box on the shaking table at the National Center for Research on Earthquake Engineering (NCREE), Taiwan. The model piles were made of stainless steel pipe and aluminum alloy pipe with an outer diameter of 101.6 mm and a wall thickness of 3.0 mm for the study of the soil-pile interactions with two kinds of stiffness of pile. Each model pile was placed in the shear box containing saturated clean fine sand. The pile tip was fixed at the bottom of the shear box to simulate the condition of a pile foundation embedded in a firm stratum. In addition, various amounts of masses were placed on the top of the piles for different conditions of superstructures. The input shakings included sinusoidal and recorded earthquake accelerations. Strain gauges and accelerometers were placed on the pile surface to obtain the behavior of the pile under shaking. The near- and far-field soil responses, including pore water pressure changes, accelerations, and settlements were also measured. The responses of the model pile and the soil-pile interactions, including the inertial and kinematic actions on the model pile, under shakings for liquefied and non-liquefied soil conditions were evaluated. The results showed that the stiffness of the soil vanished when soil liquefaction occurred. The performance of the pile foundation was affected by the relation among the dynamic characteristics of the pile and the surrounding soil, and the mass of the superstructure.

INTRODUCTION

Pile foundations had suffered extensive damage in liquefiable soils in many large earthquakes such as 1964 Niigata Earthquake, 1989 Loma Prieta Earthquake, 1995 Kobe Earthquake and 1999 Chi-Chi Earthquake. Therefore, many studies on soil-pile interactions for pile foundations in a liquefiable stratum were conducted recently in order to understand the mechanism of the dynamic loading on the piles (soil-pile interaction) and their responses under earthquake loading. The results of these studies can provide information of performance criteria for aseismic design of structures with pile foundations.

Lateral loading tests in the field or in the laboratory and shaking table tests on model piles within soil specimens, under either 1 g or centrifugal conditions, have been used to investigate the pile behaviors and soil-pile interaction in liquefiable soils (e.g. Ashford et al. 2006, Dobry & Abdoun 2001, Tokimatsu et al. 2005). This research used the large biaxial laminar shear box developed at the National Center for Research on Earthquake Engineering (NCREE) as the soil

container and instrumented model piles were installed inside the shear box filled with saturated sand. Besides lateral loading tests on the model piles, the biaxial shear box with the model pile in a saturated sand specimen was placed on the shaking table at NCREE. One- and multi-directional sinusoidal and recorded earthquake accelerations were applied from the shaking table. The soil and pile responses and their interaction, including the inertial and kinematic actions on the model pile, under these types of shakings were studied. The performances of the model piles under shaking were evaluated according to the test results

MODEL PILES AND SAND SPECIMEN

Two different types of model piles were used in the shaking table tests. One was made of a stainless steel pipe, 1.50 m in length, with an outer diameter of 101.6 mm, a wall thickness of 3 mm and a flexural rigidity, EI , of 186.05 kN-m²; the other was made of an aluminum alloy pipe, 1.60 m in length, with the same diameter and wall thickness and $EI = 77.62$ kN-m².

Strain gauges and mini-accelerometers were placed at different locations to respectively measure bending moments and accelerations along the model pile. The pile was fixed at the bottom of the shear box to simulate the condition of a pile foundation embedded in rock or within a firm soil stratum. A rigid steel adapter for application of lateral force was fixed to the top of the steel pile, while up to 6 disks of masses were attached to the top of the aluminum pile to simulate various conditions of the superstructure. Each disk of mass weighs 37.10 kg. The model pile with instrumentation inside the shear box was set up before preparation of the sand specimen, as shown in Fig. 1. Figure 2 is the layout of instrumentation on the model pile and within the sand specimen.

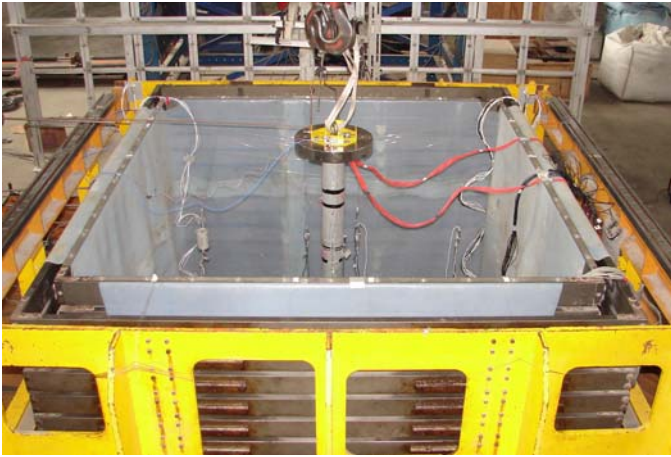


Fig. 1. The instrumented aluminum pipe with one disk of mass on the top inside the shear box.

We used clean fine silica sand from Vietnam for the sand specimen inside the laminar shear box. This sand has been used in the shaking table tests for liquefaction studies at NCREE (Ueng et al. 2006). The grain size distribution of the sand is shown in Fig. 3 and its maximum and minimum void ratios are 0.887~0.912 and 0.569~0.610, respectively. The sand specimen was prepared using the wet sedimentation method after the placement of the model pile and instruments in the shear box. The sand was rained down into the shear box filled with water to a pre-calculated depth. The size of sand specimen is 1.880 m \times 1.880 m in plane and about 1.40 m in height before shaking tests. Details of the sand specimen preparation and the mechanism of the biaxial laminar shear box were described in Ueng et al. (2006).

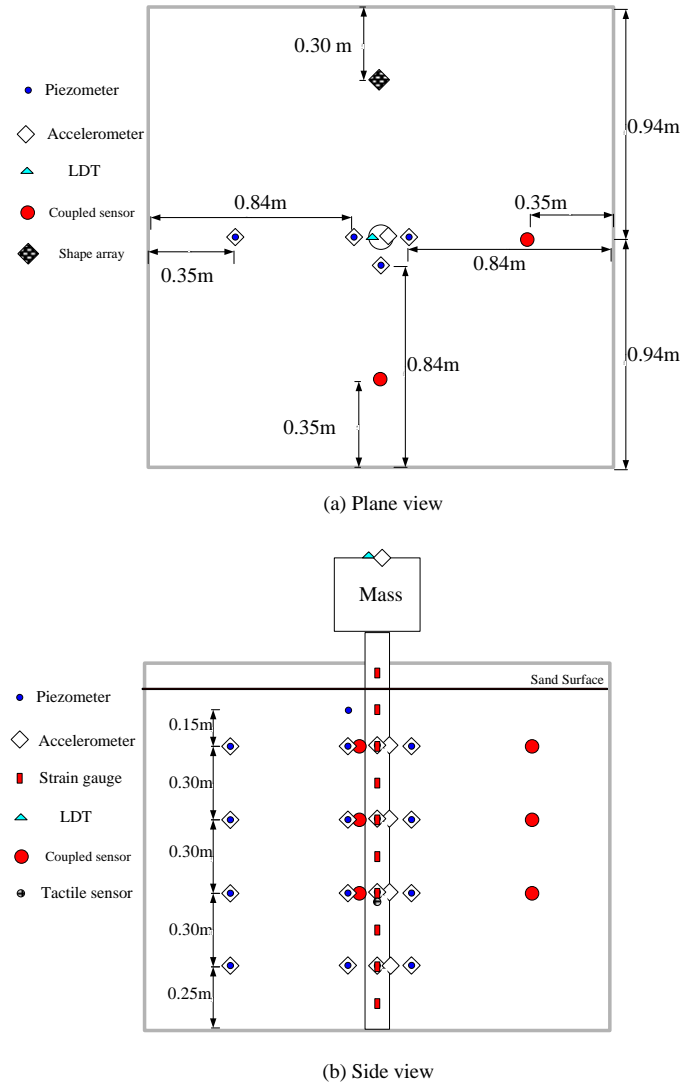


Fig. 2. Instrumentation on the model pile and within the sand specimen.

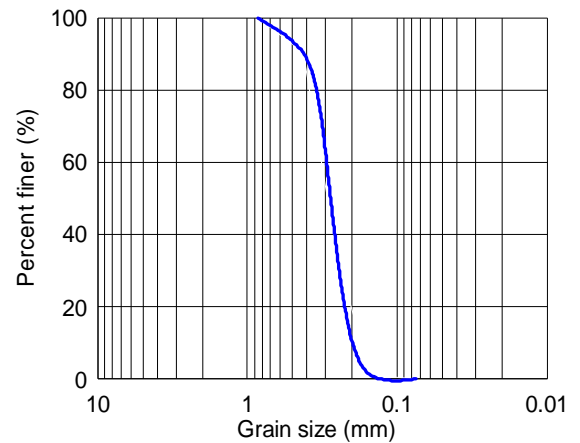


Fig. 3. Grain size distribution of Vietnam sand.

SHAKING TABLE TESTS

Shaking table tests were first conducted on each model pile without sand specimen to evaluate the dynamic characteristics of the model pile itself. Sinusoidal and white noise accelerations with amplitudes from 0.03 to 0.075 g were applied in X- and Y-directions. The model pile within the saturated sand specimen was then tested under one- and multi-directional sinusoidal (1~24 Hz) and recorded earthquake accelerations with amplitudes ranging from 0.03 to 0.25 g. White noise accelerations were also applied in both X- and Y-directions to investigate the behaviors of the model pile and the sand specimen with amplitude of 0.03 g. Figure 4 shows a shaking table test of the aluminum model pile with 6 disks of masses on its top in the sand specimen.

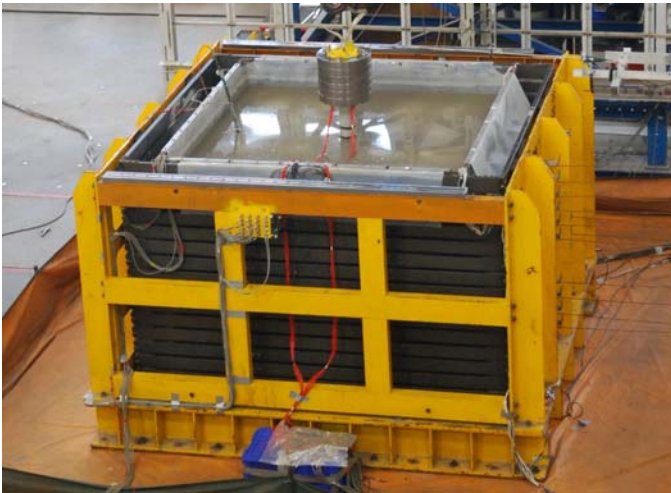


Fig. 4. The model pile with mass on its top in saturated sand specimen on the shaking table.

Pile top displacements, strains and accelerations at different depths on the pile, and pore water pressures and accelerations in the sand specimen (near field and far field) were measured during each shaking, as shown in Fig. 2. Besides, the frame movements at different depths of the laminar shear box were also recorded to evaluate the responses and liquefaction of the sand specimen using displacement transducers and accelerometers as shown in Fig. 5. Pore water pressures inside the sand specimen were measured continuously until sometime after the end of shaking to observe the dissipation of the water pressures. The height of the sand surface after each test was obtained for the settlement and density of the sand specimen. Soil samples were taken using short thin-walled cylinders at different depths and locations after completion of the shaking tests to obtain the densities of the sand specimen.

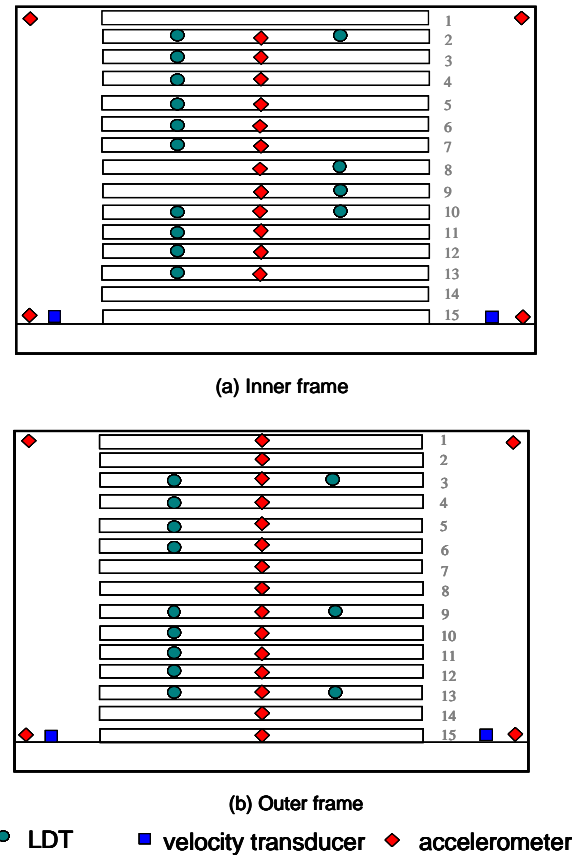


Fig. 5. Instrumentation on the laminar shear box.

TEST RESULT ANALYSES

Dynamic characteristics of model piles

Shaking table tests on the model pile without sand specimen were conducted to evaluate the dynamic characteristics of the model pile. We consider the behavior of model pile on shaking table as a single-degree viscously damped system as shown in Fig. 6. We observe the response of free vibration at the end of the input motion to estimate the natural frequency and damping ratio of the model pile. According to the analyses of a series of shaking table tests, the natural frequency of the steel pile with an adapter on the pile top ranges from 13.2 to 13.67 Hz, and the average damping ratio is about 1.6 %. Furthermore, the dynamic characteristics of the model piles can also be evaluated based on the forced vibration of white noise shaking. The amplification curve was derived from the Fourier spectral ratio of the measured acceleration of the pile top to that of the input motion. The predominant frequency of the steel pile was identified at about 13.62 Hz as shown in Fig. 7. The identified predominant frequencies by these two methods are almost the same. Table 1 lists the predominant frequencies of the steel and aluminum model piles according to the test data.

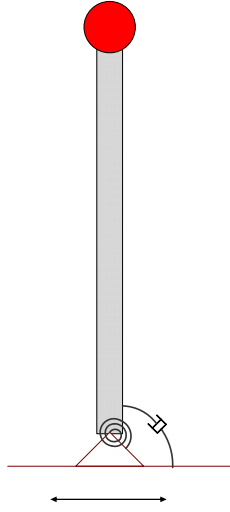


Fig. 6. Schematic drawing of the single-degree viscously damped system.

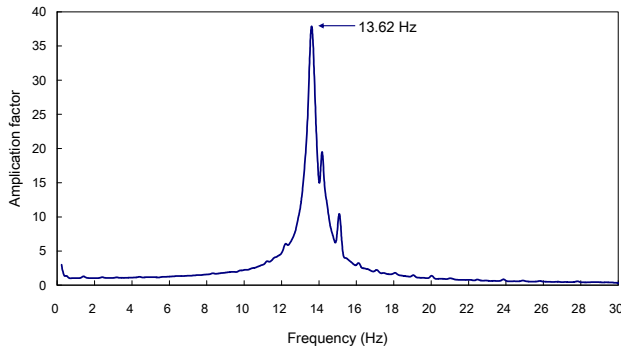


Fig. 7. Amplification factor vs. frequency for the steel pile from white noise shaking.

Table 1. Predominant frequencies of the model piles

Mass on pile top	Steel pile	Aluminum pile
	Freq., Hz	Freq., Hz
No mass	-	23.4
Rigid adapter	13.62	-
1 disk of mass	-	5.55
3 disks of masses	-	3.11
6 disks of masses	-	2.03

Dynamic characteristics of soil and soil-pile system under small amplitude of shakings

The dynamic characteristics of soil stratum and soil-pile system were evaluated by a series of shaking table tests on the model pile within the saturated sand specimen with small amplitude. Figure 8 shows the amplification factors between the steel pile top and the far-field ground surface under the white noise accelerations and sinusoidal vibrations of various

frequencies with amplitude of 0.03 g. Results obtained under sinusoidal shakings of various frequencies are also shown in Fig. 8. In addition, the predominant frequencies of both far-field soil and the combined pile-soil system are nearly the same with a value of about 11.5 Hz.

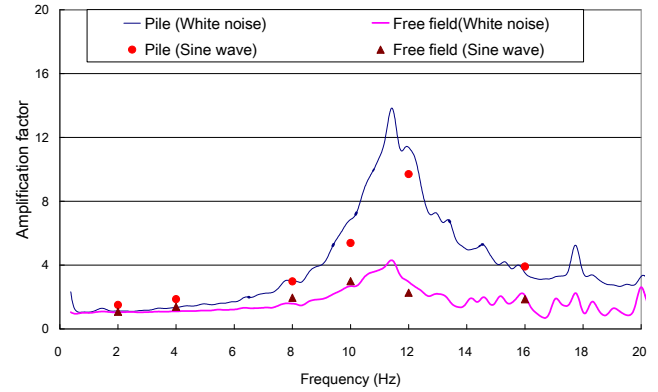


Fig. 8. Amplification factor vs. frequency for far-field soil and steel pile ($D_r = 37.13\%$)

Table 2 lists the predominant frequencies of soil and soil-pile system in sand specimens of different densities for the case of the steel model pile. It can be seen that the predominant frequencies of soil and soil-pile system are almost the same and these frequencies increase with relative density of the soil specimen. This infers that the kinematic force from the soil motion dominates the pile response because of the small inertia force from the superstructure.

Table 2. The predominant frequencies of soil and soil-pile system for the steel pile in different soil densities

Density of soil D_r , %	Predominant frequency, Hz	
	Soil	Pile in soil
37.13	11.5	11.5
50.78	12.5	12.38
70.58	12.9	12.9

Table 3 lists the predominant frequencies of soil and soil-pile system for the aluminum pile in soil of various relative densities. It can be found that, for the model pile without mass and with one disk of mass, the predominant frequencies of both soil and the soil-pile system are almost the same and these frequencies increase with the relative density of the soil specimen. For the pile with 6 disks of masses, the predominant frequency of soil-pile system is significantly lower than that of the soil specimen. Comparing the predominant frequencies of the aluminum pile without and within soil specimen (Table 1 and Table 3, respectively,) one can find that, except for the case without mass on the pile top, the predominant frequencies of the model pile in the soil specimen were higher than those without soil due to the constraint of the soil on the pile. For small inertia force from the superstructure (e.g. no mass or 1 disk of mass on the pile top), pile response was dominated by

the kinematic force from the soil motion, but for large inertia force (e.g. 6 disks of masses on the pile top), the response of pile was mainly governed by the inertia force from the superstructure. Therefore, these observations suggest that the mass and inertia force induced by the superstructure may play an important role on the soil-pile interaction.

Table 3. Predominant frequencies of soil and soil-pile system for the aluminum pile in the soil specimen of different relative densities

Mass on pile top	Soil-Pile Freq., Hz	Soil Freq., Hz	Dr %
No mass	10.49	10.49	7.5
No mass	11.7	11.68	30.6
1 disk of mass	11.7	11.8	31.7
1 disk of mass	11.7	11.8	40.5
6 disks of masses	4.88	13.1	56.6
6 disks of masses	5.1	13.2	64.7

Figure 9 shows the amplification curves of the aluminum pile with 6 disks of masses on the top and far-field ground surface under the white noise accelerations with amplitude of 0.03 g. It can be seen that there are two distinct frequencies causing higher amplification of the pile top motions. One is the predominant frequency of the soil-pile system and the other is the predominant frequency of the soil specimen. It is obvious that, in this case, the inertia effect of the pile and the added mass is more pronounced than the kinematic effect of the soil movement on the pile behavior under shaking. More tests and analyses are needed to evaluate the relative importance of the kinematic and inertia effects on the soil-pile interaction and the pile performance during earthquakes.

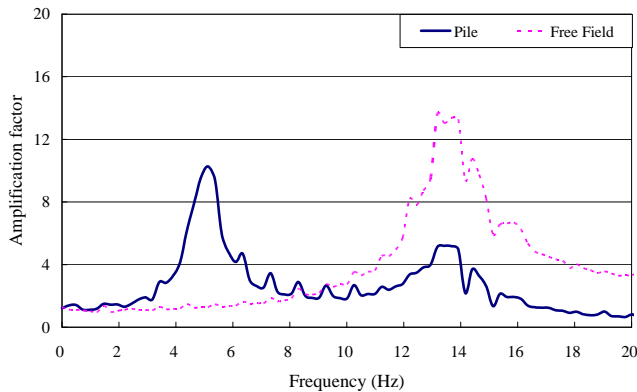


Fig. 9. Amplification factor vs. frequency for far-field soil and aluminum pile with 6 disks of masses (Dr = 64.7 %)

Response of model piles in liquefiable soil

Figure 10 shows time histories of accelerations and displacements of the steel pile and accelerations of the free-field soil and excess pore water pressure ratios (r_u) at various depths in the specimen during one-dimensional sinusoidal shaking with frequency of 8 Hz and amplitude of 0.05 g. It can

be seen that the accelerations of pile and soil increase with height due to the upward shear wave propagation. The depth of liquefaction was determined based on the measurements of mini-piezometers in the sand specimen and accelerometers on the inner frames (Ueng et al. 2009). In this test, the liquefied depth of sand specimen was about 0.53 m from the sand surface. According to the time history of excess pore water pressure ratio (r_u) (Fig. 11(d)), the liquefaction occurs in the shallower depth (≈ 0.136 m) at about 1.3 s after the beginning of shaking, and progressed to the final liquefaction depth (0.53 m) at around 3.0 s after start of shaking. At the same time, the accelerations of pile and soil within the liquefied depth reduced slightly in magnitude and became irregular while those in the non-liquefied zone remained unchanged. Such behavior was due to the loss of stiffness of the soil when liquefaction occurred.

Figure 11 shows the measured time histories of accelerations and displacements of the aluminum pile with 6 masses on its top and accelerations of the free-field soil and excess pore water pressure ratios (r_u) at various depths in the sand specimen during one-dimensional sinusoidal shaking with frequency of 4 Hz and amplitude of 0.15 g, respectively. In this shaking, the sand specimen was fully liquefied at about 3.1 second. It was found that the maximum accelerations along the pile occurred before liquefaction of the sand specimen. After liquefaction, the accelerations of the pile reduced and remain steady while the accelerations of the soil diminished. In addition, the maximum displacement occurred before liquefaction reached the final depth and the amplitude of displacement decreased and remained steady afterwards with the same shaking frequency as the input motion. This phenomenon can be interpreted as that the stiffness of the soil almost vanished when the specimen was fully liquefied. The reason might be attributed to the lower predominant frequency of the aluminum pile with masses because of the lack of soil constraint.

The amplification curve of the aluminum pile top with 6 disks of masses during the post-liquefaction period was shown in Fig. 12. It was found that the predominant frequency of the model pile within liquefied soil was identified at around 2 Hz. Comparing the predominant frequency of the aluminum pile with 6 disks of masses on its top and without soil specimen (Table 1), one can find that the predominant frequency of the model pile within liquefied soil was almost the same as that of model pile without soil specimen. This clearly demonstrates that the stiffness of the soil almost vanished when soil liquefaction occurred.

The above mentioned pile behaviors can be explained as follows. Prior to soil liquefaction, the frequency of the soil-pile system was closer to the exciting frequency from the shaking table and there was amplification of the pile motions under shaking. When liquefaction occurred and soil lost its strength and stiffness, the nature frequency of the pile without soil constraint was quite different from that of the external exciting motions. This resulted in a smaller induced steady

motion of the pile with the same frequency of the input motion. These results suggest that the acceleration and displacement of the pile during soil liquefaction may depend on the relation between the frequency of the pile and that of the excitation. In other words, to reasonably evaluate the seismic behavior of structure system, the dynamic characteristics of the super-structure, foundation and soil stratum should be taken into consideration together. In addition, the stability of the pile-structure system should be determined according to the depth of liquefaction, the conditions of superstructure and the load capacity of the pile foundation.

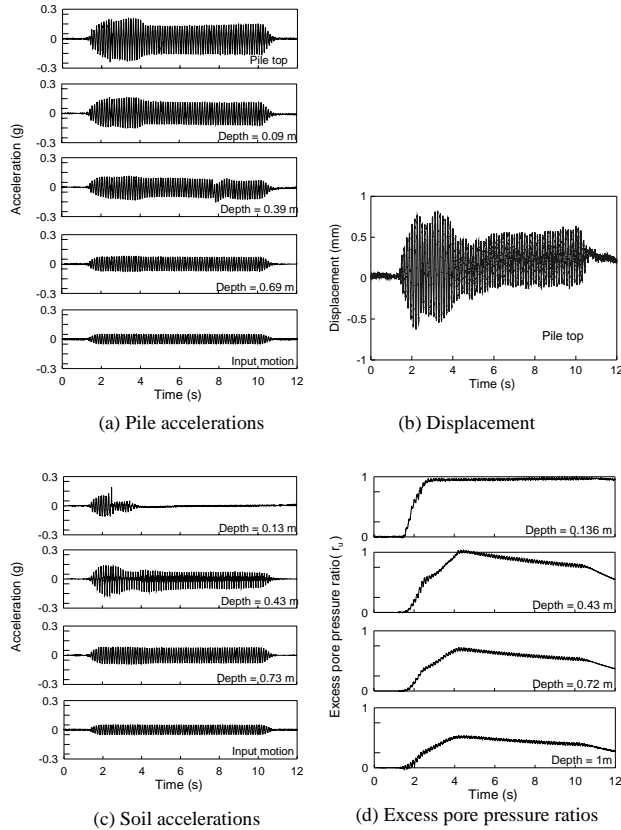


Fig. 10. Time histories of accelerations of the steel pile and the free-field soil, pile top displacement and excess pore pressure ratios in the sand specimen ($Dr = 59.4\%$)

CONCLUSIONS

Shaking table tests were conducted on a steel and an aluminum model piles in the biaxial laminar shear box with and without saturated sand specimen. The displacements, strains and accelerations at different depths of the model piles were measured. The analyses of the dynamic behavior of the model piles and the pile-soil system during shaking tests were conducted based on the test results. It was found that the behavior of the model piles under shaking was affected by the soil specimen density, the dynamic characteristics of the piles

and the surrounding soil, and the mass of the superstructure. Further tests and analyses of the test data will be performed to understand the soil-pile interaction, such as the relationship of ground reaction on the pile, and pore water pressure generation versus pile displacements and their coupling.

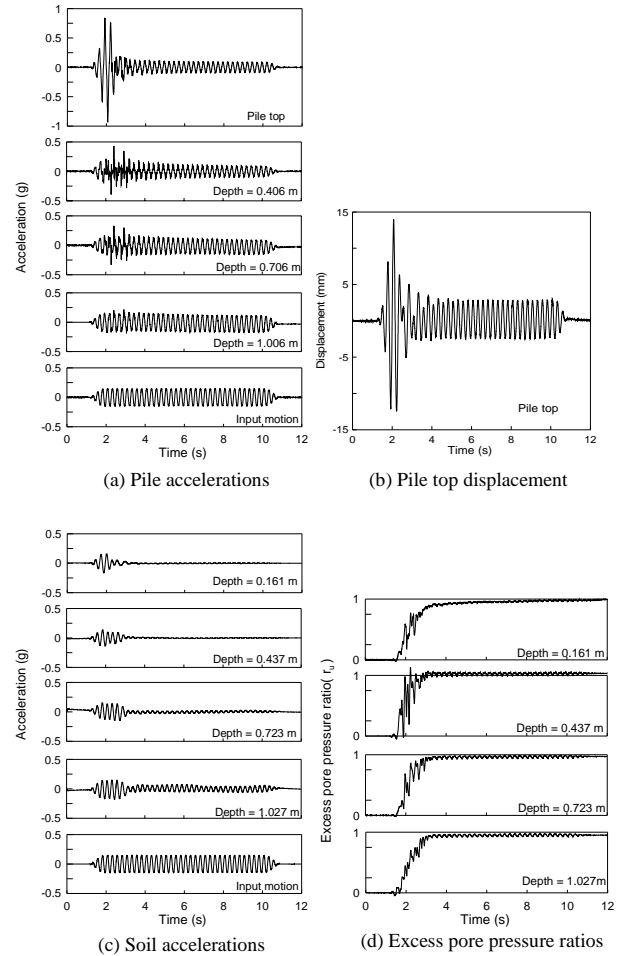


Fig. 11. Time histories of accelerations of the aluminium pile and the free-field soil, pile top displacement and excess pore pressure ratios in the sand specimen ($Dr = 68.6\%$)

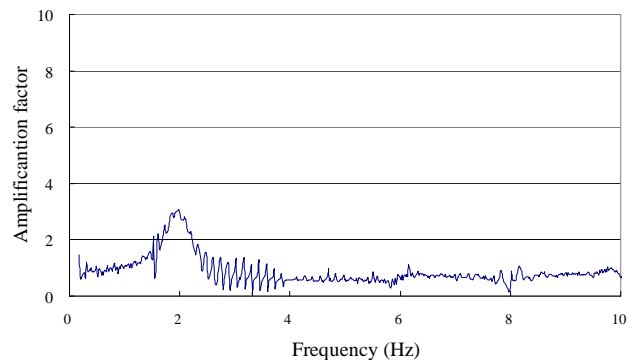


Fig. 12. Amplification factor vs. frequency for aluminum pile with 6 disks of masses after initial liquefaction ($Dr = 68.6\%$)

ACKNOWLEDGEMENTS

This study is supported by NCREC, Taiwan. The technical supports and operational assistances in the shaking table testing including large specimen preparation by the graduate students from National Taiwan University and National Taiwan Ocean University and the engineers at NCREC are gratefully acknowledged. The authors also thank the assistances of Prof. W. J. Chang and Mr. S. Y. Chueh from National Chi Nan University in conducting data acquisition and synchronization.

REFERENCES

Ashford, S.A., T. Juirnarongrit, T. Sugano and M. Hamada [2006]. "Soil-pile Response to Blast-induced Lateral Spreading I: Field Test", *Geotechnical and Geoenvironmental Engng.*, Vol.132, No. 2, pp. 152-162.

Dobry, R.D. and T. Abdoun [2001]. "Recent Studies on Seismic Centrifuge Modeling of Liquefaction and Its Effect on Deep Foundations" State-of-the-Art Report (SOAP3), *Proc. 4th Intern. Conf. on Recent Adv. in Geo. Erthq. Engrg. and Soil Dyn.*, San Diego, CA, March 26-31, Vol. 2.

Tokimatsu, K., H. Suzuki and M. Sato [2005]. "Effect of Inertial and Kinematic Interaction on Seismic Behavior of Pile with Embedded Foundations", *Soil Dyn. and Earthquake Engng.*, Vol. 25, No. 7-10, pp. 753-762.

Ueng, T.S., M.H. Wang, M.H. Chen, C.H. Chen and L.H. Peng [2006]. "A Large Biaxial Shear Box for Shaking Table Tests on Saturated Sand", *Geotechnical Testing Journal*, Vol. 29, No. 1, pp. 1-8.

Ueng, T.S., C.W. Wu, H.W. Cheng and C.H. Chen [2009]. "Settlements of Saturated Clean Sand Deposits in Shaking Table Tests", Submitted for publication.